

Differential Apaf-1 levels allow cytochrome *c* to induce apoptosis in brain tumors but not in normal neural tissues

Carrie E. Johnson*, Yolanda Y. Huang^{†‡}, Amanda B. Parrish*, Michelle I. Smith^{†‡}, Allyson E. Vaughn^{†‡}, Qian Zhang[§], Kevin M. Wright^{†‡}, Terry Van Dyke[§], Robert J. Wechsler-Reya*, Sally Kornbluth*[¶], and Mohanish Deshmukh^{†‡¶}

*Department of Pharmacology and Cancer Biology, Duke University Medical Center, Durham, NC 27708; and [†]Neuroscience Center and Departments of [‡]Cell and Developmental Biology and [§]Genetics, University of North Carolina, Chapel Hill, NC 27599

Edited by Tak Wah Mak, University of Toronto, Toronto, Canada, and approved November 12, 2007 (received for review September 24, 2007)

Brain tumors are typically resistant to conventional chemotherapeutics, most of which initiate apoptosis upstream of mitochondrial cytochrome *c* release. In this study, we demonstrate that directly activating apoptosis downstream of the mitochondria, with cytosolic cytochrome *c*, kills brain tumor cells but not normal brain tissue. Specifically, cytosolic cytochrome *c* is sufficient to induce apoptosis in glioblastoma and medulloblastoma cell lines. In contrast, primary neurons from the cerebellum and cortex are remarkably resistant to cytosolic cytochrome *c*. Importantly, tumor tissue from mouse models of both high-grade astrocytoma and medulloblastoma display hypersensitivity to cytochrome *c* when compared with surrounding brain tissue. This differential sensitivity to cytochrome *c* is attributed to high Apaf-1 levels in the tumor tissue compared with low Apaf-1 levels in the adjacent brain tissue. These differences in Apaf-1 abundance correlate with differences in the levels of E2F1, a previously identified activator of Apaf-1 transcription. ChIP assays reveal that E2F1 binds the Apaf-1 promoter specifically in tumor tissue, suggesting that E2F1 contributes to the expression of Apaf-1 in brain tumors. Together, these results demonstrate an unexpected sensitivity of brain tumors to postmitochondrial induction of apoptosis. Moreover, they raise the possibility that this phenomenon could be exploited therapeutically to selectively kill brain cancer cells while sparing the surrounding brain parenchyma.

astrocytoma | caspase | cell death | medulloblastoma | neurons

Primary brain tumors arise from cells intrinsic to the brain and intracranial cavity. Although these tumors account for only a small percentage of cancers, they cause a disproportionate share of cancer-related morbidity and mortality (1). Despite resection in conjunction with chemoradiation, the 5-year survival rate for glioblastoma, the most common histologic subtype, remains only 3% (2). Although survival rates for childhood medulloblastoma are better, long-term neurological deficits secondary to radiation therapy remains a significant problem (3). Therefore, therapeutic strategies that selectively induce apoptosis in brain tumors while sparing surrounding neural tissue could offer significant clinical promise.

Apoptosis is a form of programmed cell death required for proper embryonic development and tissue homeostasis. Aberrant signaling allows malignant cells to evade apoptosis, thus fostering tumor progression (4). In the intrinsic pathway of apoptosis, death-inducing signals converge upon the mitochondria, causing release of cytochrome *c*. Cytosolic cytochrome *c* binds to Apaf-1, leading to recruitment of procaspase-9 and formation of the apoptosome. Apoptosome-mediated activation of caspase-9 activates executioner caspase-3 and caspase-7, which promote cell death (5).

Cytosolic cytochrome *c* is sufficient to induce apoptosis in many dividing cells, including fibroblasts, HEK293, and HeLa (6, 7). In contrast, differentiated sympathetic neurons are highly resistant to apoptosis induced by cytochrome *c* (8). This differ-

ential susceptibility to cytochrome *c*-induced death in cycling cells and neurons led us to hypothesize that activating apoptosis with cytochrome *c* might selectively induce death in dividing brain tumor cells while sparing neurons in the brain parenchyma. However, this idea was tempered by the fact that various tumors have been shown to differ markedly in their sensitivity to cytochrome *c*. Although ovarian cancers and melanomas appear resistant to cytochrome *c*-induced apoptosis (9, 10), breast cancers are hypersensitive to cytochrome *c* (11).

We show here that, despite the remarkable resistance of mature neurons and brain tissues to cytochrome *c*, both high-grade astrocytoma and medulloblastoma are susceptible to cytochrome *c*-mediated apoptosis. Importantly, although normal brain exhibits nearly undetectable levels of Apaf-1, we demonstrate that brain tumors express high levels of Apaf-1 through transcriptional induction of Apaf-1 mRNA. These results identify direct activation of the apoptosome as a potential therapeutic strategy for brain tumors that would eliminate cancer cells while sparing surrounding neural tissue.

Results

Multiple Types of Neurons Become Resistant to Cytochrome *c* upon Maturation. We recently reported that decreased Apaf-1-dependent apoptosome activity, which accompanies neuronal differentiation, renders sympathetic neurons resistant to cytochrome *c*-mediated apoptosis (8). To determine whether the development of cytochrome *c* resistance is seen in other neurons, including those in the CNS, we examined neurons from the dorsal root ganglion (DRG), cerebellum, and cortex. Because these neurons mature at different times, we chose two time points for each neuronal type, corresponding to early and late stages of differentiation. Sensory neurons from the DRG were isolated from embryonic day 15 (E15) and postnatal day 2 (P2) mice. Microinjection of cytochrome *c* into E15 DRG neurons after 1 day in culture (E16 equivalent) induced extensive death within 3 h. In contrast, P2 DRG neurons injected after 1 day in culture (P3 equivalent) were remarkably resistant to cytochrome *c* (Fig. 1A).

To examine the sensitivity of cerebellar granule neurons (CGN) and cortical neurons to cytochrome *c*, we used a cell-free assay, as the small size of these neurons is unsuitable for microinjection. In this assay, addition of cytochrome *c* to cyto-

Author contributions: C.E.J. and Y.Y.H. contributed equally to this work; C.E.J., Y.Y.H., A.B.P., M.I.S., A.E.V., K.M.W., S.K., and M.D. designed research; C.E.J., Y.Y.H., A.B.P., M.I.S., A.E.V., and K.M.W. performed research; Q.Z., T.V.D., and R.J.W.-R. contributed new reagents/analytic tools; C.E.J., Y.Y.H., A.B.P., M.I.S., A.E.V., K.M.W., S.K., and M.D. analyzed data; and C.E.J., Y.Y.H., S.K., and M.D. wrote the paper.

The authors declare no conflict of interest.

This article is a PNAS Direct Submission.

[¶]To whom correspondence may be addressed. E-mail: kornb001@mc.duke.edu or mohanish@med.unc.edu.

© 2007 by The National Academy of Sciences of the USA

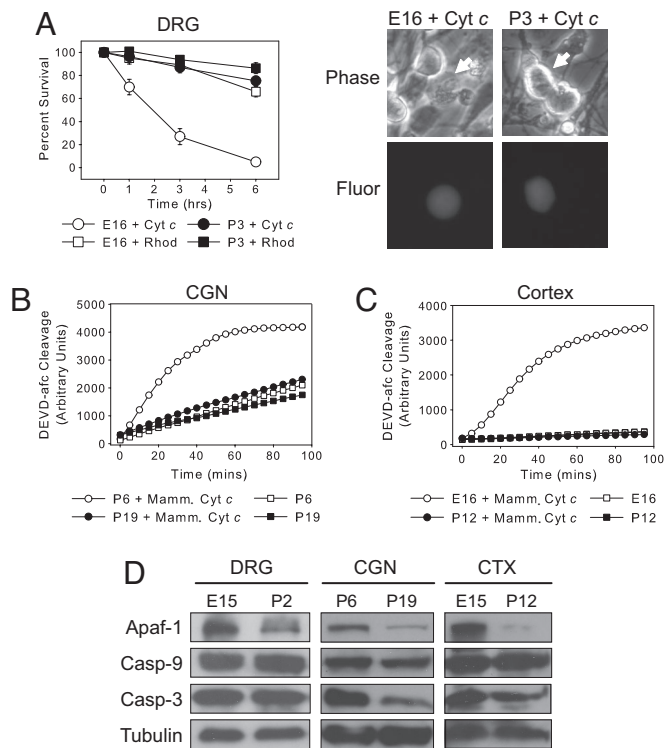


Fig. 1. Cytochrome *c* is incapable of activating caspases and inducing apoptosis in mature neurons. (A) E16 and P3 neurons from DRG were microinjected with 10 $\mu\text{g}/\mu\text{l}$ cytochrome *c* and rhodamine dextran (for visualization). Data shown are neuronal survival at times after injection and are mean \pm SEM of three independent experiments. In corresponding images, arrows indicate microinjected cells. (Magnification: $\times 400$.) (B and C) Cytosolic lysates from CGN (B) and whole cortex (CTX) (C) at early and late stages of neuronal maturation were assessed for caspase activation after the addition of 10 μM cytochrome *c*. Caspase activation was monitored via cleavage of DEVD-afc. Yeast cytochrome *c*, which cannot bind Apaf-1 (8), was added to extracts as a negative control. (D) Immunoblotting shows protein levels of Apaf-1, caspase-9, and caspase-3 in DRG, CGN, and whole cortex at early and late stages of neuronal differentiation.

solic lysates (extracts) prepared from either primary tissue or cultured cells can recapitulate caspase-dependent apoptosis (6). Although cytochrome *c* induced robust caspase activation in extracts of P5 CGN maintained 1 day in culture (P6 equivalent), no significant caspase activation was detected in extracts of P5 CGN maintained 14 days in culture (P19 equivalent) (Fig. 1B). Next, we examined whether cortical extracts exhibited a similar resistance to cytochrome *c* with maturation. Addition of cytochrome *c* was sufficient to activate caspases in cortical extracts from E16 but not P12 mice (Fig. 1C). Together, these results show that our previous observations in sympathetic neurons, in which cytochrome *c* sensitivity is dramatically decreased upon maturation, can be generalized to multiple neuronal cell types, including those of the CNS.

To determine whether the resistance to cytochrome *c* upon neuronal maturation correlated with Apaf-1 down-regulation, we examined components of the apoptotic machinery in early and late stages of neuronal differentiation. Immunoblot analysis confirmed that, in all neuronal cell types examined, Apaf-1 levels were high in early-stage neurons but markedly decreased with maturation (Fig. 1D).

Cytochrome *c* Induces Robust Caspase Activation in Brain Tumor Cells. Unlike in neurons, in many dividing cells the introduction of cytosolic cytochrome *c* induces apoptosis. This difference

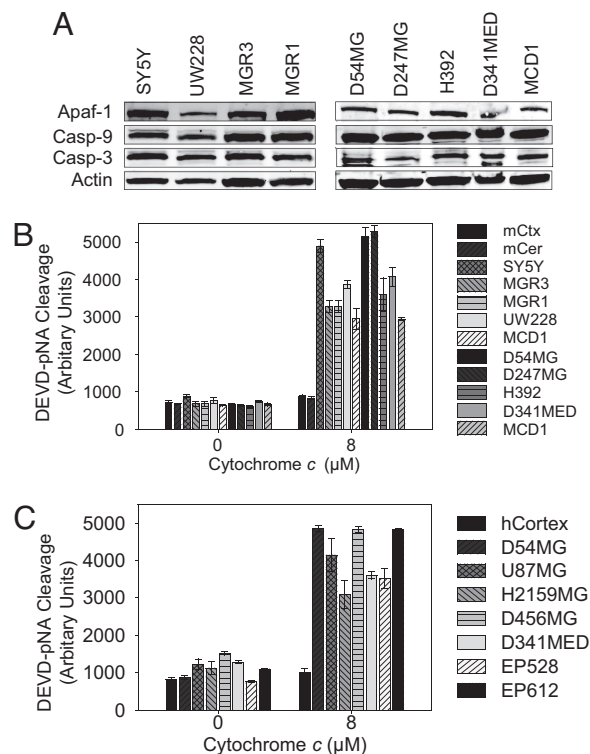


Fig. 2. Brain cancer cells are hypersensitive to cytochrome *c*-induced apoptosis. (A) Protein levels of Apaf-1, caspase-9, and caspase-3 were examined in human brain tumor cell lines by immunoblotting. SY5Y, neuroblastoma; UW228, D341MED, and MCD1, medulloblastoma; MGR3, MGR1, D54MG, D247MG, and H392, glioblastoma. (B) Extracts from human brain tumor cell lines or mouse neural tissue were supplemented with 8 μM cytochrome *c*. Caspase activation was monitored via cleavage of Ac-DEVD-pNA. Data shown are mean \pm SEM of three independent experiments. mCtx, mouse cortex; mCer, mouse cerebellum. (C) Extracts from human non-neoplastic temporal cortex and xenograft tumors were assessed for their ability to activate caspases as in B. U87MG and D54MG, adult glioma; H2159MG and D456MG, pediatric glioma; D341MED, medulloblastoma; EP528 and EP612, ependymoma.

prompted us to investigate whether brain tumors would be sensitive to cytochrome *c* while surrounding neural tissue would be resistant. We first confirmed that components of the apoptotic machinery were present in extracts from neuroblastoma (SH-SY5Y), medulloblastoma (UW228, D341MED, MCD1), and glioblastoma (MGR3, MGR1, D54MG, D247MG, H392) cell lines (Fig. 2A). Next, we found that cytochrome *c* elicited robust caspase activation in all of the brain tumor cell line-derived extracts, but not in extracts of mouse cortex or cerebellum (Fig. 2B).

As an alternative to working with cultured cells, we examined whether human brain tumor cells grown *s.c.* in immunocompromised mice also exhibited cytochrome *c* sensitivity. Xenograft extracts were prepared from human medulloblastoma (D341MED), human glioma from adults (D54MG, U87MG) and children (H2159MG, D456MG) and ependymoma (EP528, EP612). Consistent with the cultured cell data, addition of cytochrome *c* to the xenograft extracts elicited marked caspase activation. In contrast, extract from adult human cortex did not induce caspase activation upon cytochrome *c* addition (Fig. 2C).

Endogenous Mouse Models of High-Grade Astrocytoma and Medulloblastoma Demonstrate Selective Cytochrome *c*-Induced Caspase Activation in Tumor Tissue. To extend relevance of these results to brain tumor models where spontaneously forming lesions within

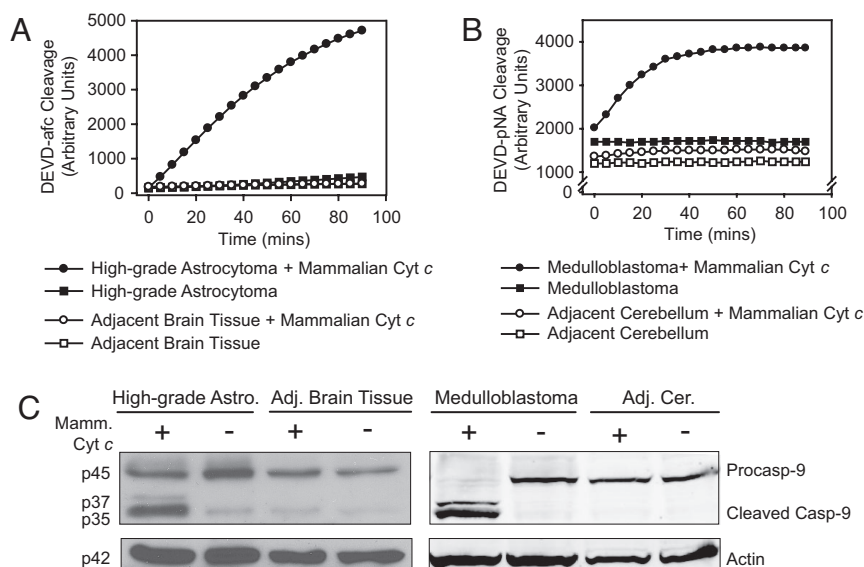


Fig. 3. Brain tumors from mouse models of high-grade astrocytoma and medulloblastoma display sensitivity to cytochrome *c*-mediated apoptosis. (A and B) Extracts prepared from tumor tissues and adjacent neural tissues of two brain tumor mouse models, high-grade astrocytoma (A) and medulloblastoma (B), were supplemented with cytochrome *c* and caspase activation was monitored. (C) Immunoblotting shows caspase-9 cleavage in extracts treated in A and B. Astro., astrocytoma; Adj. Cer., adjacent cerebellum.

the brain more accurately mimic human disease, we examined whether cytochrome *c* could induce caspase activation in tumors from both high-grade astrocytoma and medulloblastoma mouse models. These models enabled us to compare tumor tissue with surrounding neural tissue from the same animal. In the high-grade astrocytoma model, mice have been engineered to achieve somatic pRb inactivation and constitutive K-ras^{G12D} activation with or without PTEN deletion, specifically in adult astrocytes. Tumors from these mice have been histopathologically characterized as predominantly anaplastic astrocytoma (WHO grade III) or glioblastoma (WHO grade IV) (Q.Z., C. R. Miller, C. Yin, C. Y. Yang, E. Bullitt, K. D. McCarthy, T. Jacks, D. N. Louis, and T.V.D., unpublished data). Extracts from these tumors exhibited strong caspase activation upon addition of cytochrome *c*, whereas extracts prepared from adjacent neural tissue did not (Fig. 3A). Next, we examined the ability of cytochrome *c* to activate caspases in tumors from *patched* heterozygous mice that develop medulloblastoma (12, 13). Caspases were activated in medulloblastoma extracts after cytochrome *c* addition, whereas no caspase activation was detected in extracts of adjacent cerebellar tissue (Fig. 3B). Consistent with apoptosis-mediated apoptosis, caspase-9 processing was observed in both high-grade astrocytoma and medulloblastoma extracts supplemented with cytochrome *c*, but not in extracts prepared from adjacent neural tissue (Fig. 3C). These data illustrate the potential of cytochrome *c* to activate caspases selectively in brain tumors *in vivo*.

Apaf-1 Expression Levels Determine the Differential Sensitivity to Cytochrome *c* in Normal and Malignant Brain Tissue. In considering the molecular basis for the differential cytochrome *c* sensitivity of brain tumor and normal brain tissue, we reflected on our earlier observations that cytochrome *c* resistance in differentiated sympathetic neurons was caused by low Apaf-1 levels (8). Low Apaf-1 expression was also observed in mature cerebellar and cortical neurons (Fig. 1D) (14). In contrast, Apaf-1 expression was clearly evident in the brain cancer cell lines (Fig. 2B). Importantly, Apaf-1 immunoblotting revealed markedly higher Apaf-1 protein levels in both high-grade astrocytoma and medulloblastoma tumors compared with adjacent neural tissues

(Fig. 4A). A similar difference was observed in human high-grade gliomas compared with normal human cortex (Fig. 4D).

To investigate whether differences in Apaf-1 expression were responsible for the differential sensitivity to cytochrome *c*, we added recombinant Apaf-1 protein to extracts prepared from late-stage CGNs, adult mouse cortex and cerebellum. Although no caspase activation was observed with cytochrome *c* alone, the addition of Apaf-1 and cytochrome *c* was sufficient to induce caspase activation (Fig. 4B). Likewise, human cortical extracts showed caspase activation with cytochrome *c* and Apaf-1 but not with cytochrome *c* alone (Fig. 4E).

We wanted to determine whether the low levels of Apaf-1 were sufficient to activate caspases in the mature brain if caspase inhibition by the inhibitor of apoptosis proteins (IAPs) was relieved. Addition of Smac, an IAP inhibitor, to extract from WT adult mouse cortex did not promote increased caspase activation (Fig. 4C). Additionally, extracts of XIAP^{-/-} and WT adult mouse cortex displayed similar resistance to cytochrome *c* (and similar sensitivity upon Apaf-1 addition) (Fig. 4C). These data illustrate that the low levels of Apaf-1 in adult mouse cortex (Fig. 4C) and cerebellum (data not shown) could not induce caspase activation even upon inactivation or removal of IAPs.

Levels of Apaf-1 in Normal and Malignant Brain Tissue Are Transcriptionally Regulated. Having found that levels of Apaf-1 protein underlie the observed sensitivity to cytochrome *c*, we examined whether this difference could be traced back to transcriptional regulation. Quantitative RT-PCR revealed that Apaf-1 mRNA was significantly more abundant in medulloblastoma than in adjacent cerebellum (Fig. 5A). Importantly, Apaf-1 mRNA levels in isolated medulloblastoma cells were comparable with developing P7 cerebellum, which is comprised of granule cell precursors; levels in both were significantly higher than in mature cerebellum (Fig. 5A).

We then investigated Apaf-1 mRNA abundance in human astrocytomas by analyzing data from published gene profiling studies available in the Oncomine Gene Profiling Database. Analysis of data from Sun *et al.* (15) demonstrated a statistically significant increase in Apaf-1 mRNA levels in glioblastoma compared with brain from epilepsy patients (Fig. 5B). In two

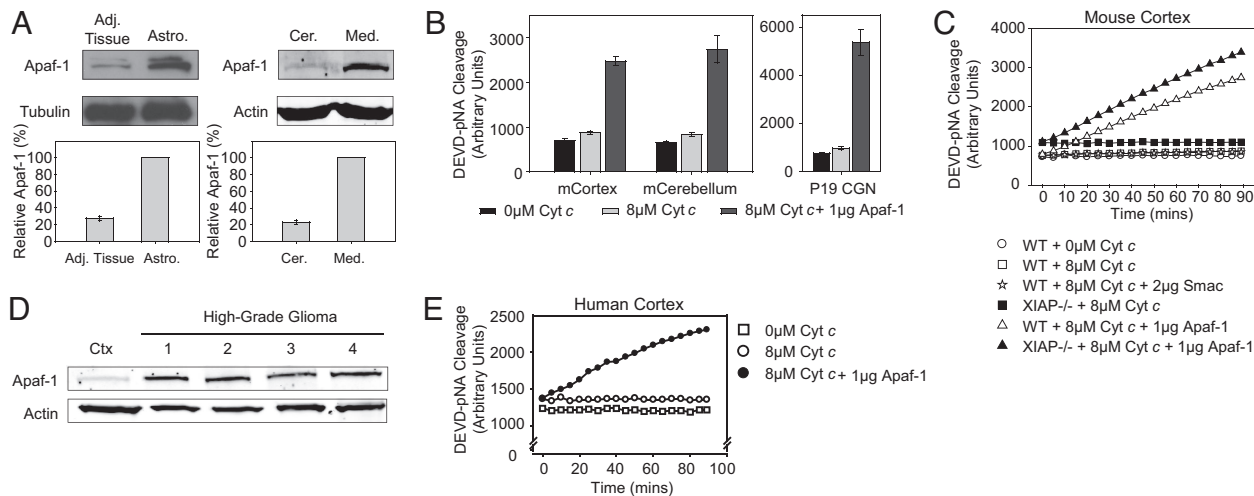


Fig. 4. A marked increase in Apaf-1 causes the increased sensitivity of brain tumor tissues to cytochrome c-mediated apoptosis. (A) Immunoblots demonstrating Apaf-1 protein levels in high-grade astrocytoma (Astro.) and medulloblastoma (Med.) relative to their respective adjacent neural tissue (Cer.: cerebellum). Quantitation of Apaf-1 (mean \pm SEM of three independent experiments) is shown. (B) Caspase activation in extracts from mouse cortex, cerebellum, and P19 CGNs was assessed in the presence of no cytochrome c, 8 μ M cytochrome c, or 8 μ M cytochrome c along with 1 μ g of recombinant Apaf-1. (C) *In vitro* assay assessing caspase activation in mouse cortical extracts when IAPs were inactivated (by Smac addition) or when XIAP was genetically removed (XIAP^{-/-}). (D) Immunoblots showing relative Apaf-1 levels in human cortex (Ctx) versus four samples of high-grade gliomas. (E) Caspase activation assay on human cortical extracts in the presence of no cytochrome c, 8 μ M cytochrome c, or 8 μ M cytochrome c along with 1 μ g of recombinant Apaf-1.

additional studies (16, 17), relative Apaf-1 mRNA expression was increased in glioblastoma (grade IV astrocytoma) compared with grade III astrocytoma (Fig. 5B). Similarly, a human tissue dot blot revealed a marked increase in Apaf-1 protein expression from a low-grade astrocytoma to a glioblastoma (Fig. 5C). These data suggest not only that Apaf-1 expression is differentially regulated in normal versus tumor cells, but also that Apaf-1 expression increases with increasing tumor grade.

To elucidate the mechanism of Apaf-1 mRNA up-regulation in brain tumors, we examined the levels of E2F1 and p53, two previously identified transcriptional activators of Apaf-1 (18–20). Levels of E2F1, but not p53, were consistently up-regulated in tumor tissues and low in adjacent brain tissues (Fig. 5D). Additionally, many tumors, including two of the brain tumor lines we analyzed (MGR1 and MCD1), have mutations in p53 (ref. 21 and Francis Ali-Osman, personal communication). We

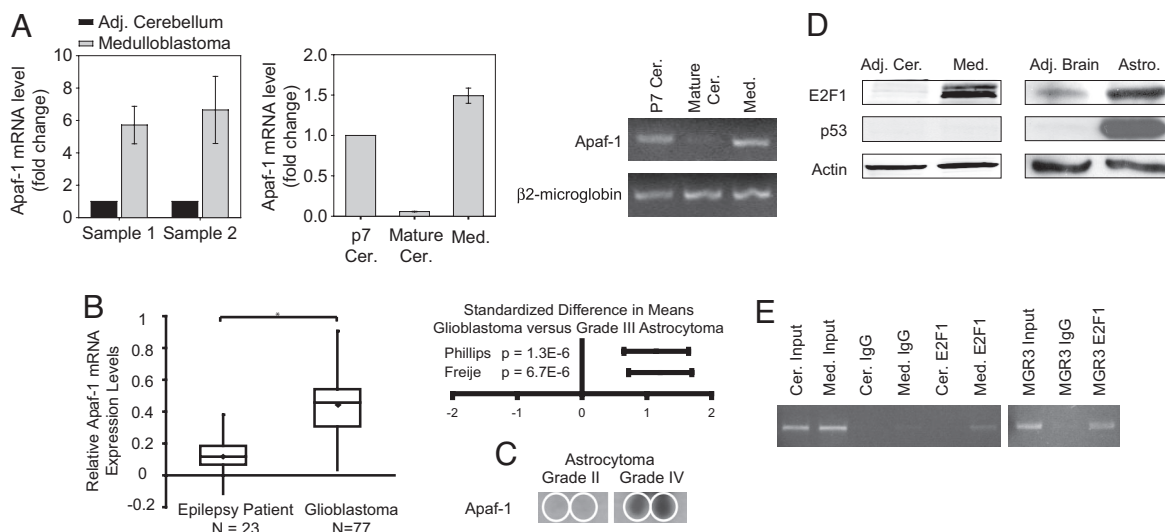


Fig. 5. Transcriptional regulation of Apaf-1 mRNA levels contributed by E2F1. (A) Quantitative analysis from RT-PCR shows the fold changes of Apaf-1 mRNA from dissected medulloblastoma and adjacent cerebellar tissues. Cells isolated from medulloblastoma tumor (Med.) were compared with normal P7 and adult cerebellar tissue. Data display the fold changes of Apaf-1 mRNA relative to normal P7 cerebellum, which is arbitrarily set as 1, and a corresponding agarose gel is shown for the PCR. (B) Oncomine analysis of three independent gene profiling studies, with data from Sun *et al.* (15) used to compare Apaf-1 mRNA expression levels in brain from epilepsy patients and in glioblastoma (*, $P < 0.0001$, independent two-tailed *t* test) and with data from Phillips *et al.* (17) and Freije *et al.* (16) analyzed by using the Comprehensive Metaanalysis software to plot the standardized difference in means along with the 95% confidence intervals for Apaf-1 mRNA in grade III astrocytoma (corresponds to 0 on the x axis) compared with glioblastoma (positive values indicate an increase in Apaf-1 expression in glioblastoma versus grade III astrocytoma). (C) A human tissue dot blot with duplicated samples demonstrates Apaf-1 levels in grade II astrocytoma and glioblastoma. Areas within the white circles represent sample location. (D) Immunoblotting shows levels of E2F1 and p53 in brain tumor tissues versus adjacent brain tissue from mouse models of medulloblastoma and high-grade astrocytoma. (E) ChIP assay demonstrates E2F1 association with Apaf-1 promoter in mouse medulloblastoma tissue and in the human glioblastoma cell line MGR3.

therefore focused on determining whether E2F1 was associated with the Apaf-1 promoter in brain tumors. Indeed, ChIP assays demonstrated that E2F1 specifically associates with the Apaf-1 promoter in mouse medulloblastoma tissue and the human glioblastoma cell line MGR3 (Fig. 5E). In aggregate, the coordinated up-regulation of E2F1 and Apaf-1 in brain tumor cells, the previously reported ability of E2F1 to drive Apaf-1 transcription, and the ability of E2F1 to bind Apaf-1 promoter in brain tumors all suggest that E2F1 contributes to Apaf-1 expression in brain tumors.

Discussion

Low Apaf-1 Levels Offer Protection from Cytochrome *c*-Dependent Apoptosis in Differentiated Neurons and Neural Tissue. Resistance to cytochrome *c*-induced apoptosis in neuronally differentiated rat pheochromocytoma PC12 cells and differentiated sympathetic neurons has been reported (8). In this study, we show that this striking development of resistance to cytochrome *c* during maturation is seen in multiple types of neurons, including those of the CNS. Specifically, we demonstrate this resistance in isolated late-stage neurons (Fig. 1) and extracts from adult mouse cortex and cerebellum (Fig. 2B) and human cortex (Fig. 2C).

We have examined the mechanistic basis for this neuronal resistance to cytochrome *c*-mediated apoptosis and identified a link between Apaf-1 expression levels and the developmental state of a neuron. As neurons mature they dramatically decrease their levels of Apaf-1. Reconstitution with recombinant Apaf-1 protein in late-stage neurons and mature neural tissue (Fig. 4 B and E) restores sensitivity to cytochrome *c*-induced apoptosis, thus providing strong evidence that down-regulation of Apaf-1 is the critical factor underlying the observed apoptotic resistance.

Similarly, other studies in rodent brain (14, 22) and mouse retina (23) have reported that neuronal maturation leads to inhibition of apoptosis, which parallels a decrease in Apaf-1 expression. We theorize that the reduction in Apaf-1 levels accompanying neuronal maturation may be a way of restricting unwanted apoptosis in differentiated neurons, in which long-term survival is necessary. Thus, up-regulation of Apaf-1 is predicted to be necessary and sufficient for these neurons to undergo cytochrome *c*-mediated apoptosis under pathological conditions. Indeed, during DNA damage-induced neuronal death (18, 24) and after fluid percussion-induced traumatic brain injury (14), Apaf-1 levels were markedly increased.

Brain Tumor Susceptibility to Cytochrome *c*-Induced Apoptosis. Although inhibition of apoptosis is a hallmark of cancer, different cancers use distinct mechanisms to serve this purpose. In some instances, cancer cells evade apoptosis by preventing mitochondrial cytochrome *c* release in response to apoptotic stimuli. Other tumors display resistance to cytoplasmic cytochrome *c* because of defective apoptosome formation (25, 26). In contrast, we have previously shown that breast cancers are actually hypersensitive to cytochrome *c*-induced apoptosis relative to normal mammary epithelial cells (11).

Given this unexpected phenomenon in breast cancer cells, we decided to investigate the sensitivity of primary brain tumors to cytochrome *c*-induced apoptosis. Using cultured human brain tumor cells (Fig. 2B), human brain cancer-derived xenograft tumors (Fig. 2C), and *in vivo* mouse models of high-grade astrocytoma and medulloblastoma (Fig. 3), we found that, unlike their normal counterparts, brain tumors are susceptible to cytochrome *c*-induced apoptosis. Our mouse model data confirm this differential sensitivity between tumor tissue and adjacent neural tissue despite common genetic alterations in both tissues in the engineered mice. Although the sensitivity of breast and brain cancers to cytochrome *c* is superficially similar, the underlying mechanisms governing this sensitivity appear to be

entirely distinct. Specifically, breast cancer cytochrome *c* hypersensitivity reflects overexpression of the apoptosome activator PHAPI, without alterations in levels of core apoptosome components (11). However, we report here that brain tumor sensitivity to cytochrome *c* is controlled through elevation of Apaf-1 expression relative to the extremely low levels present in mature neurons and neural tissue (Fig. 4).

Moreover, this difference in Apaf-1 is transcriptionally regulated (Fig. 5A). Of note, OncoPrint analysis of publicly available microarray data suggests that Apaf-1 mRNA levels are not only higher in glioblastoma relative to normal brain, but also that Apaf-1 mRNA levels increase with increasing tumor grade (Fig. 5B). It may be that, because Apaf-1 transcription can be regulated by E2F1, increased Apaf-1 levels are an inexorable consequence of the increased E2F1 levels associated with (and in part responsible for) increased proliferation in tumor cells. According to this model, we would expect elevated Apaf-1 levels in poorly differentiated, highly proliferative brain tumors, which we did indeed observe in comparing glioblastoma (grade IV astrocytoma) with well differentiated grade II astrocytoma (Fig. 5C). Furthermore, expression of E2F1 has recently been shown to be sufficient to cause brain tumors in mice (27). Here, we show that brain tumors harbor high levels of E2F1, whereas levels in normal brain are quite low (Fig. 5D). Furthermore, our ChIP studies suggest a physiological role for E2F1 in promoting Apaf-1 transcription in brain tumors (Fig. 5E).

Although Apaf-1 can be regulated at the transcriptional level, it has been reported previously that Apaf-1 translation initiates via an internal ribosomal entry segment (IRES) (28). One known factor in IRES-mediated Apaf-1 translation, nPTB, is expressed in neuronal cell lines (29, 30). Therefore, keeping Apaf-1 protein levels low in mature neurons may critically depend on keeping Apaf-1 mRNA levels low. It is attractive to speculate that neurons are poised to translate Apaf-1 should the message be produced, for example, under conditions of neuronal damage where reinstatement of Apaf-1-dependent apoptosis might be desirable.

Apoptosome Activation as a Therapeutic Strategy. In aggregate, our data show that activating apoptosis with cytochrome *c* induces caspase activation in brain tumors but not in mature neural tissue. We have demonstrated that this differential sensitivity to cytochrome *c* is caused by a transcriptionally regulated difference in Apaf-1 levels. Although apoptotic resistance upstream of mitochondrial cytochrome *c* release likely renders brain tumors refractory to standard chemotherapeutics, our results show that they remain sensitive to apoptosis induced by cytochrome *c*.

Exploiting this vulnerability by directly activating the apoptosome with peptides or small molecules that mimic cytochrome *c* is therefore an attractive therapeutic approach for cancer cells that maintain functionally active apoptosome components. Importantly, our results from extracts of neural tissue, which are comprised of both neurons and glia, suggest that, like mature neurons, glia are also likely to be resistant to cytochrome *c*. Therefore, we believe that the development of a cytochrome *c* mimetic would be particularly beneficial in the context of brain tumors where it would selectively induce apoptosis in tumor cells while sparing adjacent brain tissue.

Because local delivery of a cytochrome *c* mimetic would be necessary to avoid potential systemic side effects, wafer implant technology would be one feasible approach. During brain tumor excision, gel wafers embedded with chemotherapeutics are inserted into the space previously occupied by tumor, resulting in slow release of drug precisely in the region of persisting malignant cells (31). Ongoing studies are focused on the development of a cytochrome *c* mimetic that could be delivered in such a manner to eliminate brain tumor cells without harming surrounding neural tissue.

Materials and Methods

Cell Culture and Microinjection. Primary neurons from the DRG and the cerebellum were cultured as described (32, 33). SH-SY5Y neuroblastoma cells (gift from Daniel Sanchis, Universitat de Lleida, Lleida, Spain) were maintained in a 1:1 mixture of DMEM and Ham's F12 supplemented with 10% FBS. Glioblastoma lines, MGR1 and MGR3 (gifts from Francis Ali-Osman, Duke University), were maintained in low glucose DMEM supplemented with 10% FBS. Medulloblastoma lines UW228 (gift from John Silber, University of Washington, Seattle) and MCD1 (gift from William Freed, National Institutes of Health, Bethesda) were maintained in DMEM supplemented with nonessential amino acids, L-glutamine, and 10% FBS. Remaining glioblastoma and medulloblastoma lines were obtained from the Duke University Preston Robert Tisch Brain Tumor Center and maintained in RPMI medium 1640 supplemented with 10% FBS. Sensory neurons from the DRG were microinjected by using 10 $\mu\text{g}/\mu\text{l}$ cytochrome *c* as described (8). The microinjection solution contained 100 mM KCl, 10 mM KPI (pH 7.4), and 4 mg/ml rhodamine dextran to mark injected cells. Cell viability was determined by counting rhodamine-positive cells with intact, phase-bright cell bodies.

Extract Preparation. Cytosolic extracts from cultured neurons were prepared as described (8). Brain tumor cell lines, xenograft tumors, and human cortical tissues were harvested, washed with cold PBS, and pelleted. Pellets were resuspended in hypotonic lysis buffer [20 mM Hepes (pH 7.5), 10 mM KCl, 1.5 mM MgCl_2 , 1 mM EDTA, 1 mM EGTA, 1 mM DTT, 1 mM PMSF, 5 $\mu\text{g}/\text{ml}$ leupeptin, and 5 $\mu\text{g}/\text{ml}$ aprotinin] with 250 mM sucrose, and incubated for 15 min on ice. Tissues were homogenized by using a 0.5-ml Bellco glass homogenizer and centrifuged for 30 min at 14,000 rpm (Eppendorf 5415C) at 4°C, and the supernatant was preserved as extract. Extracts were quantitated by using the Bradford method. Xenograft tumors, human cortical tissue, and high-grade gliomas were provided by the Tisch Brain Tumor Center. Tissues were diced on ice into 1-mm³ pieces, and extracts were prepared as above. Medulloblastoma tumor cells were isolated for RT-PCR as described (12).

Caspase Assays. Assays were performed as described (8, 11). In brief, extracts were incubated with 10 μM either mammalian or yeast cytochrome *c* and 1 mM dATP at 37°C for 30 min before addition of the fluorogenic substrate, Ac-DEVD-afc (Biomol). Alternatively, extracts alone or with 8 μM cytochrome *c* were incubated as above before addition of the colorimetric substrate Ac-DEVD-pNA (Biomol).

Immunoblotting. Antibodies used include: anti-caspase-9 [M0543 (MBL International); 9504 (Cell Signaling)], anti-procaspase 3 (9665; Cell Signaling), anti-Apaf-1(13F11 and 2E12; Alexis), anti-p53 (DO1; Santa Cruz), anti-E2F1

(C-20; Santa Cruz), anti- α -tubulin (T9026; Sigma), and anti- β -actin (A5316; Sigma). Either Alexa Fluor secondary antibodies were used with the LI-Cor Odyssey IR Imaging System or HRP-conjugated secondary antibodies (Pierce Chemical) along with an ECL-Plus detection system (Amersham Biosciences). Protein array of human astrocytomas was from the BioChain Institute (A1235713-1).

Real-Time RT-PCR. RNA was isolated by using the small-scale RNAqueous Kit and treated with DNase I (Ambion). For RT-PCR, first-strand cDNA was synthesized with an oligo(dT) primer by adding $\approx 300 \mu\text{g}$ of RNA with SuperScript III Reverse Transcriptase (Invitrogen). Real-time PCR was performed by using iQ SYBR Green Supermix (BioRad), 10 μM forward and reverse primers (sequences available on request), and 5 ng of cDNA. Real-time quantitation was performed by using a BioRad iCycler iQ System. Data were normalized to β_2 -microglobulin, and fold change was determined by using the $2^{-\Delta\Delta\text{CT}}$ method (34). For RT-PCR agarose gel analysis, reactions were performed as above except with iQ Supermix.

Oncomine Microarray Data Analysis. Three independent gene profiling studies (15–17) publicly available on the Oncomine Cancer Profiling Database (www.oncomine.org) were used to investigate Apaf-1 mRNA levels. The resulting data were analyzed as described by Turley *et al.* (35). Briefly, the mean Apaf-1 expression and the SD were calculated for each study. Differences in Apaf-1 expression between epileptic patient brain and glioblastoma were displayed by using a standard box-and-whisker plot. For data from the other two studies (16, 17), we calculated the standard difference in means of Apaf-1 mRNA expression between grade III and grade IV astrocytomas by using the statistical program Comprehensive Metaanalysis (Biostat).

ChIP Assay. ChIP was performed by using the EpiQuik Tissue Chromatin Immunoprecipitation Kit (Epigentek P-2003). DNA was purified by using a QIAquick PCR purification kit (Qiagen), and PCR was performed by using iQ Supermix (BioRad). Approximately 2% of the input chromatin and 7% of the ChIP samples were used as template in each case (primer sequences available on request). Amplicons were visualized with ethidium bromide in 2.5% agarose gels.

ACKNOWLEDGMENTS. We thank Xiaodong Wang (University of Texas Southwestern, Dallas) for providing recombinant human Apaf-1; Jessica Kessler, Tracy-Ann Read, and Jack Dutton for mouse medulloblastoma dissections; and Darrell Bigner, Michael Graner, Roger McLendon, Diane Satterfield, Steve Keir, Shelley Davis, and Ian Cummings from the Preston Robert Tisch Brain Tumor Center for the xenograft tumors and human tissues. This work was supported by National Institutes of Health Grants NS42197 (to M.D.) and CA102707 (to S.K.) and the Pediatric Brain Tumor Foundation.

- Newton HB (1994) *Am Fam Physician* 49:787–797.
- Central Brain Tumor Registry of the United States (2005) *Statistical Report: Primary Brain Tumors in the United States 1998–2002* (Central Brain Tumor Registry of the United States, Chicago).
- Rutkowski DT, Kaufman RJ (2004) *Trends Cell Biol* 14:20–28.
- Hanahan D, Weinberg RA (2000) *Cell* 100:57–70.
- Daniel NN, Korsmeyer SJ (2004) *Cell* 116:205–219.
- Liu X, Kim CN, Yang J, Jemmerson R, Wang X (1996) *Cell* 86:147–157.
- Li F, Srinivasan A, Wang Y, Armstrong RC, Tomaselli KJ, Fritz LC (1997) *J Biol Chem* 272:30299–30305.
- Wright KM, Linhoff MW, Potts PR, Deshmukh M (2004) *J Cell Biol* 167:303–313.
- Wolf BB, Schuler M, Li W, Eggers-Sedlet B, Lee W, Taylor P, Fitzgerald P, Mills GB, Green DR (2001) *J Biol Chem* 276:34244–34251.
- Soengas MS, Capodici P, Polsky D, Mora J, Esteller M, Opitz-Araya X, McCombie R, Herman JG, Gerald WL, Lazebnik YA, *et al.* (2001) *Nature* 409:207–211.
- Schafer ZT, Parrish AB, Wright KM, Margolis SS, Marks JR, Deshmukh M, Kornbluth S (2006) *Cancer Res* 66:2210–2218.
- Oliver TG, Read TA, Kessler LE, Mehmeti A, Wells JF, Huynh TT, Lin SM, Wechsler-Reya RJ (2005) *Development* 132:2425–2439.
- Goodrich LV, Milenkovic L, Higgins KM, Scott MP (1997) *Science* 277:1109–1113.
- Yakovlev AG, Ota K, Wang G, Movsesyan V, Bao W-L, Yoshihara K, Faden AI (2001) *J Neurosci* 21:7439–7446.
- Sun L, Hui AM, Su Q, Vortmeyer A, Kotliarov Y, Pastorino S, Passaniti A, Menon J, Walling J, Bailey R, *et al.* (2006) *Cancer Cell* 9:287–300.
- Freije WA, Castro-Vargas FE, Fang Z, Horvath S, Cloughesy T, Liao LM, Mischel PS, Nelson SF (2004) *Cancer Res* 64:6503–6510.
- Phillips HS, Kharbada S, Chen R, Forrest WF, Soriano RH, Wu TD, Misra A, Nigro JM, Colman H, Soroceanu L, *et al.* (2006) *Cancer Cell* 9:157–173.
- Fortin A, Cregan SP, MacLaurin JG, Kushwaha N, Hickman ES, Thompson CS, Hakim A, Albert PR, Cecconi F, Helin K, *et al.* (2001) *J Cell Biol* 155:207–216.
- Moroni MC, Hickman ES, Lazzarini Denchi E, Caprara G, Colli E, Cecconi F, Muller H, Helin K (2001) *Nat Cell Biol* 3:552–558.
- Furukawa Y, Nishimura N, Furukawa Y, Satoh M, Endo H, Iwase S, Yamada H, Matsuda M, Kano Y, Nakamura M (2002) *J Biol Chem* 277:39760–39768.
- Moore KD, Dillon-Carter O, Conejero C, Poltorak M, Chedid M, Tornatore C, Freed WJ (1996) *Mol Chem Neuropathol* 29:107–126.
- Madden SD, Donovan M, Cotter TG (2007) *Int J Dev Biol* 51:415–424.
- Donovan M, Cotter TG (2002) *Cell Death Differ* 9:1220–1231.
- Vaughn AE, Deshmukh M (2007) *Cell Death Differ* 14:973–981.
- Schafer ZT, Kornbluth S (2006) *Dev Cell* 10:549–561.
- Johnstone RW, Ruefli AA, Lowe SW (2002) *Cell* 108:153–164.
- Olson MV, Johnson DG, Jiang H, Xu J, Alonso MM, Aldape KD, Fuller GN, Bekele BN, Yung WK, Gomez-Manzano C, *et al.* (2007) *Cancer Res* 67:4005–4009.
- Coldwell MJ, Mitchell SA, Stoneley M, MacFarlane M, Willis AE (2000) *Oncogene* 19:899–905.
- Mitchell SA, Spriggs KA, Coldwell MJ, Jackson RJ, Willis AE (2003) *Mol Cell* 11:757–771.
- Boutz PL, Stoilov P, Li Q, Lin CH, Chawla G, Ostrow K, Shiue L, Ares M, Jr, Black DL (2007) *Genes Dev* 21:1636–1652.
- Fleming AB, Saltzman WM (2002) *Clin Pharmacokinet* 41:403–419.
- Molliver DC, Wright DE, Leitner ML, Parsadanian AS, Doster K, Wen D, Yan Q, Snider WD (1997) *Neuron* 19:849–861.
- Miller TM, Johnson EM, Jr (1996) *J Neurosci* 16:7487–7495.
- Livak KJ, Schmittgen TD (2001) *Methods* 25:402–408.
- Turley RS, Finger EC, Hempel N, How T, Fields TA, Blobel GC (2007) *Cancer Res* 67:1090–1098.